US009927394B1

(12) **United States Patent**
Dutta et al.

(10) **Patent No.: US 9,927,394 B1**
(45) **Date of Patent: Mar. 27, 2018**

(54) **MINIATURIZED GAS SENSOR DEVICE AND METHOD**

(71) Applicant: **Ohio State Innovation Foundation**, Columbus, OH (US)

(72) Inventors: **Prabir K. Dutta**, Worthington, OH (US); **Suvra P. Mondal**, Tripura (IN)

(73) Assignee: **Ohio State Innovation Foundation**, Columbus, OH (US)

(*) Notice: Subject to any disclaimer, the term of this patent is extended or adjusted under 35 U.S.C. 154(b) by 0 days.

(21) Appl. No.: **15/693,266**

(22) Filed: **Aug. 31, 2017**

Related U.S. Application Data

(62) Division of application No. 14/212,006, filed on Mar. 14, 2014.

(60) Provisional application No. 61/801,106, filed on Mar. 15, 2013.

(51) **Int. Cl.**

G01N 7/00	(2006.01)
G01N 21/00	(2006.01)
G01N 27/00	(2006.01)
G01N 27/417	(2006.01)
G01N 33/00	(2006.01)

(52) **U.S. Cl.**
CPC ***G01N 27/417*** (2013.01); ***G01N 33/0031*** (2013.01); ***G01N 33/0037*** (2013.01)

(58) **Field of Classification Search**
CPC G01N 7/00; G01N 21/00; G01N 27/00; G01N 31/00; G01N 33/00; G01N 27/26
USPC 422/83, 98; 73/23.2; 204/421, 424, 431, 204/196.09; 436/106, 116, 117, 118
See application file for complete search history.

(56) **References Cited**

U.S. PATENT DOCUMENTS

4,294,679	A	10/1981	Maurer et al.	
5,071,526	A	12/1991	Pletcher et al.	
5,841,021	A	11/1998	De Castro et al.	
6,277,267	B1	8/2001	Geloven et al.	
6,663,756	B2	12/2003	Lee et al.	
9,164,080	B2	10/2015	Dutta et al.	
2003/0121780	A1 *	7/2003	Dutta	C04B 35/486 204/424

(Continued)

FOREIGN PATENT DOCUMENTS

KR	100843169	B1	7/2008
WO	2009049091	A2	4/2009

OTHER PUBLICATIONS

Gad-El-Hak, "MEMS Design and Fabrication," The MEMS Handbook, Second Edition, 2006, Taylor & Francis Group, LLC, pp. 1-15.

(Continued)

Primary Examiner — Brian J. Sines
(74) *Attorney, Agent, or Firm* — Meunier Carlin & Curfman LLC

(57) **ABSTRACT**

Various embodiments of a gas sensor device and method of fabricating a gas sensor device are provided. In one embodiment a gas sensor device includes a base substrate, an electrolyte layer disposed on the base substrate and a plurality of potentiometric sensor units electrically coupled to the base substrate. Each potentiometric sensor unit includes an electrolyte layer disposed on the base substrate, a sensing electrode comprising tungsten oxide (WO_3) and platinum (Pt), a reference electrode comprising Pt, and a plurality of connectors coupled to the plurality of potentiometric sensors to connect the plurality of potentiometric sensors in series.

9 Claims, 13 Drawing Sheets

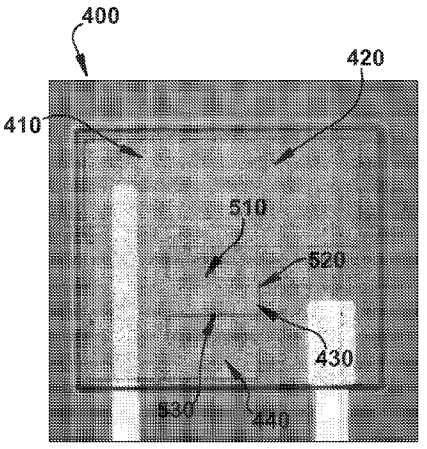

(56) **References Cited**

U.S. PATENT DOCUMENTS

2004/0074285	A1	4/2004	Dimeo, Jr. et al.	
2005/0016848	A1*	1/2005	Sahimi	G01N 27/4071 204/427
2005/0051511	A1	3/2005	Ke et al.	
2005/0214170	A1	9/2005	Kading	
2007/0114130	A1	5/2007	Lankheet et al.	
2007/0289870	A1*	12/2007	Nair	G01N 27/4062 204/424
2009/0026076	A1	1/2009	Yang	
2009/0065370	A1*	3/2009	Nair	G01N 33/0054 205/781
2010/0264900	A1	10/2010	Blackburn et al.	
2012/0247186	A1*	10/2012	Sanjeeb	G01N 33/0037 73/31.05
2013/0075255	A1	3/2013	Moon et al.	

OTHER PUBLICATIONS

Hunter et al., "Smart Sensor Systems for Human Health Breath Monitoring Applications," Journal of Breath Research, 2011, vol. 5, pp. 1-11.

PCT International Search Report and Written Opinion for PCT/US2014/027889, dated Jun. 30, 2014, pp. 1-17.

* cited by examiner

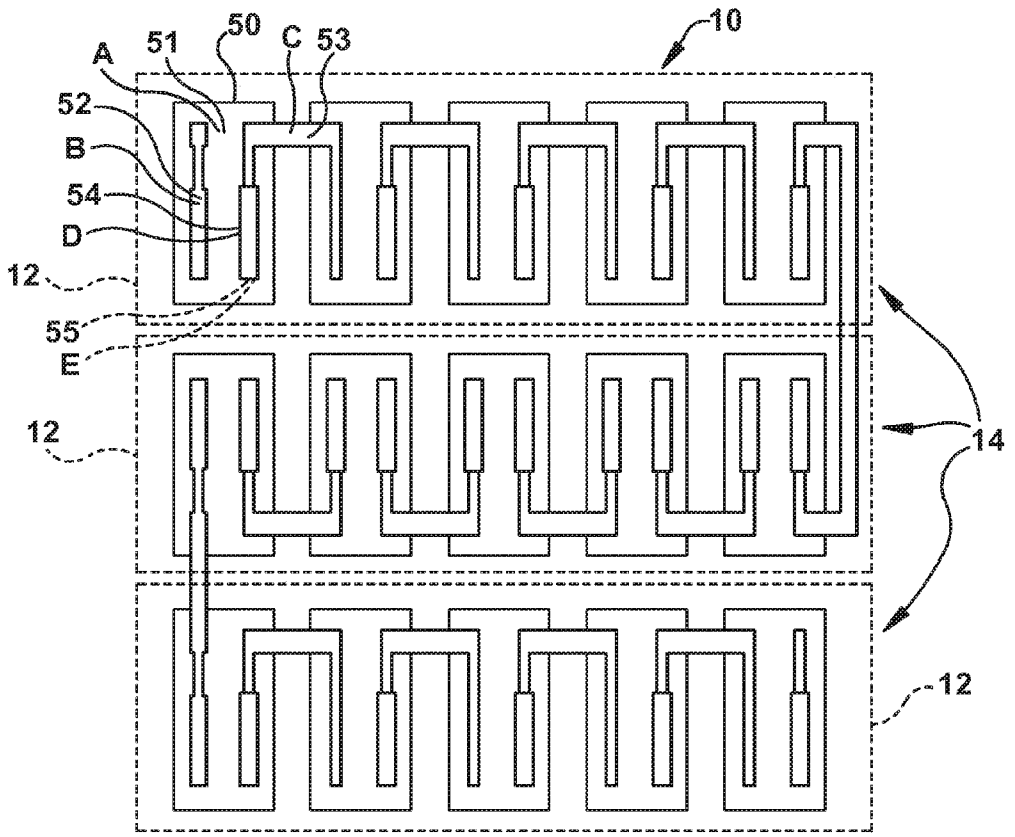
10
A
51
50
C
53
52
B
54
D
12
55
E
12
14
12

Fig. 1

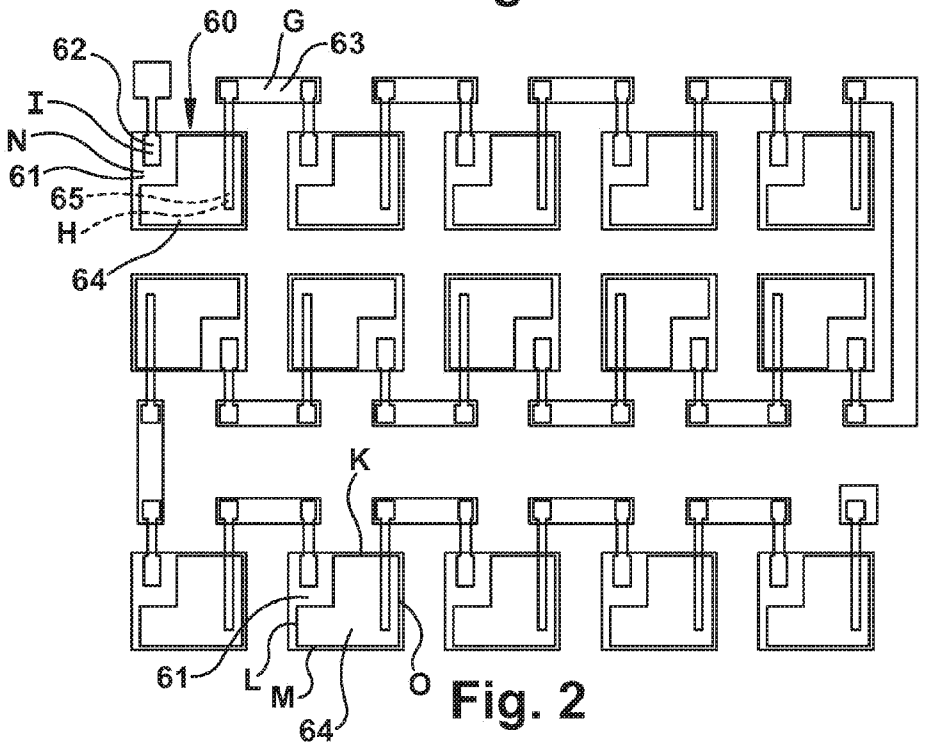
60
G
62
63
I
N
61
65
H
64
K
61
L
M
64
O

Fig. 2

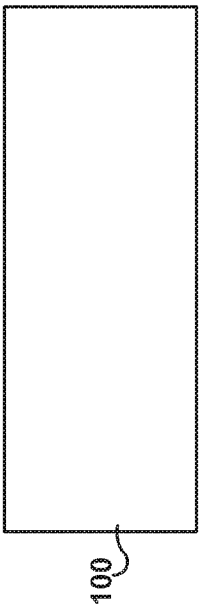

Fig. 3b

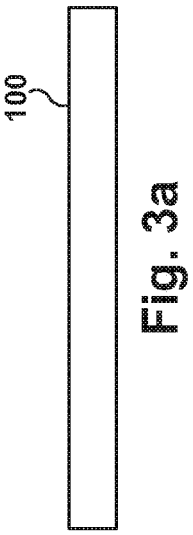

Fig. 3a

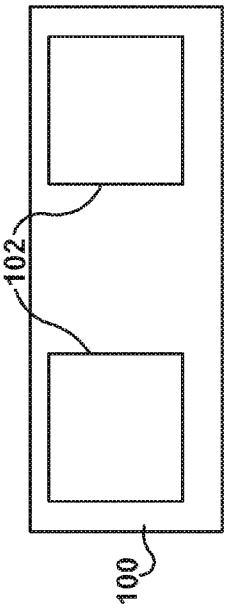

Fig. 4b

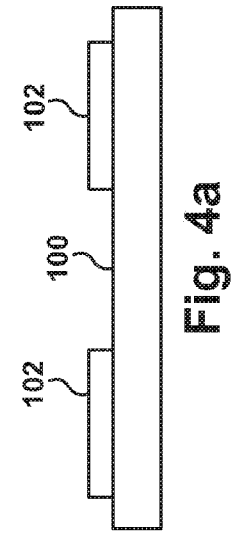

Fig. 4a

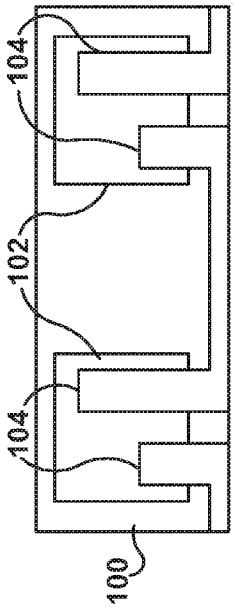

Fig. 5b

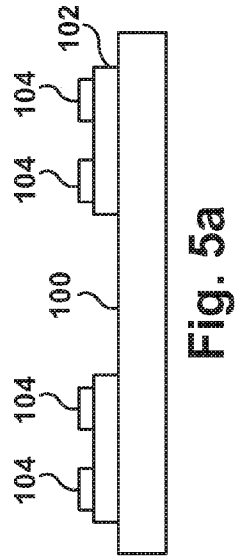

Fig. 5a

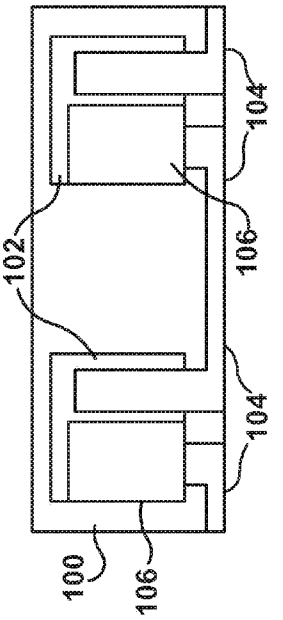

Fig. 6b

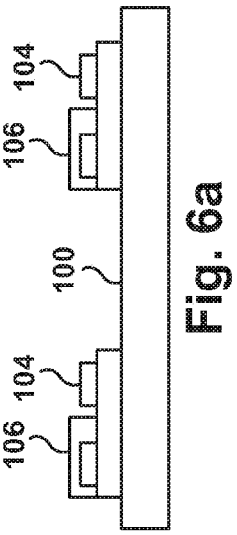

Fig. 6a

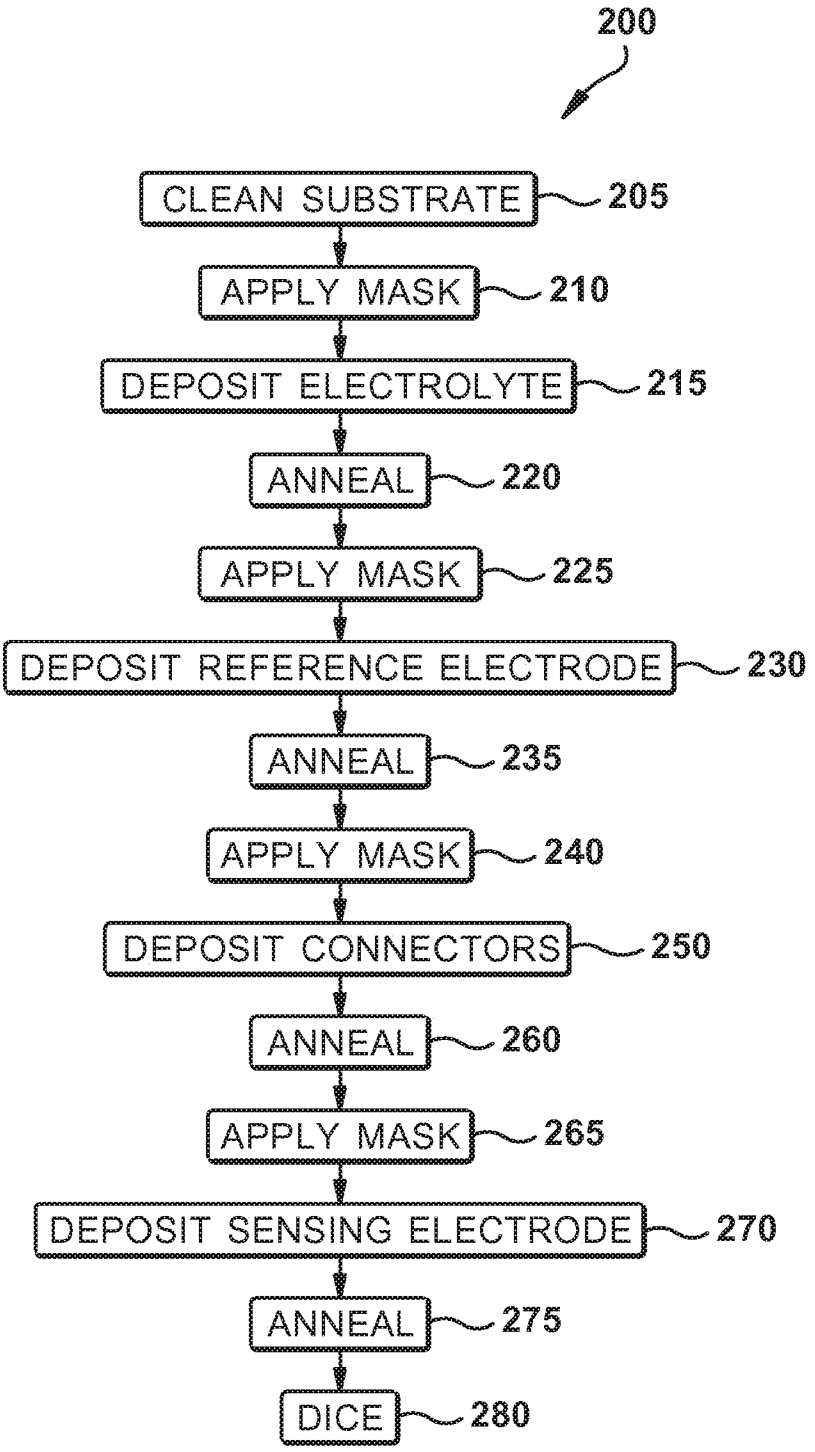
200
CLEAN SUBSTRATE
205
APPLY MASK
210
DEPOSIT ELECTROLYTE
215
ANNEAL
220
APPLY MASK
225
DEPOSIT REFERENCE ELECTRODE
230
ANNEAL
235
APPLY MASK
240
DEPOSIT CONNECTORS
250
ANNEAL
260
APPLY MASK
265
DEPOSIT SENSING ELECTRODE
270
ANNEAL
275
DICE
280

Fig. 7

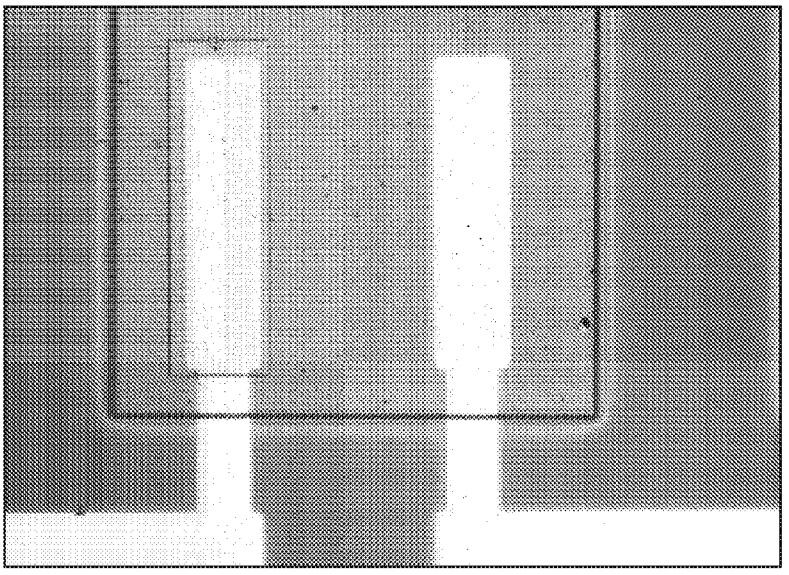

Fig. 8

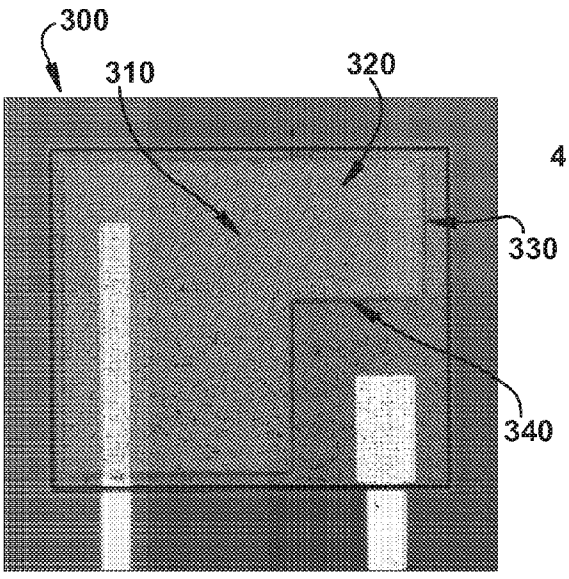

Fig. 9

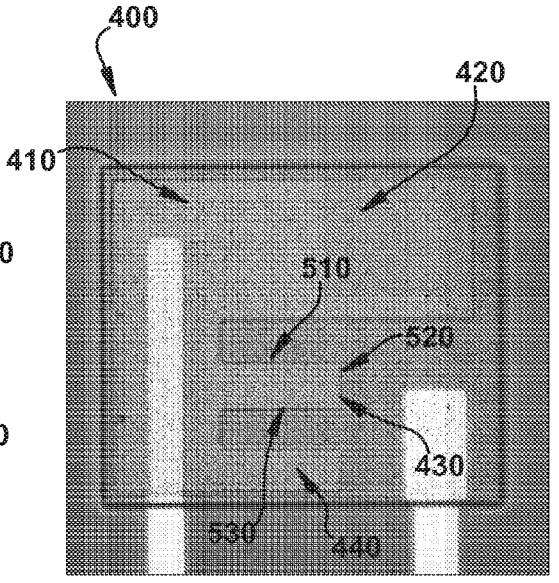

Fig. 10

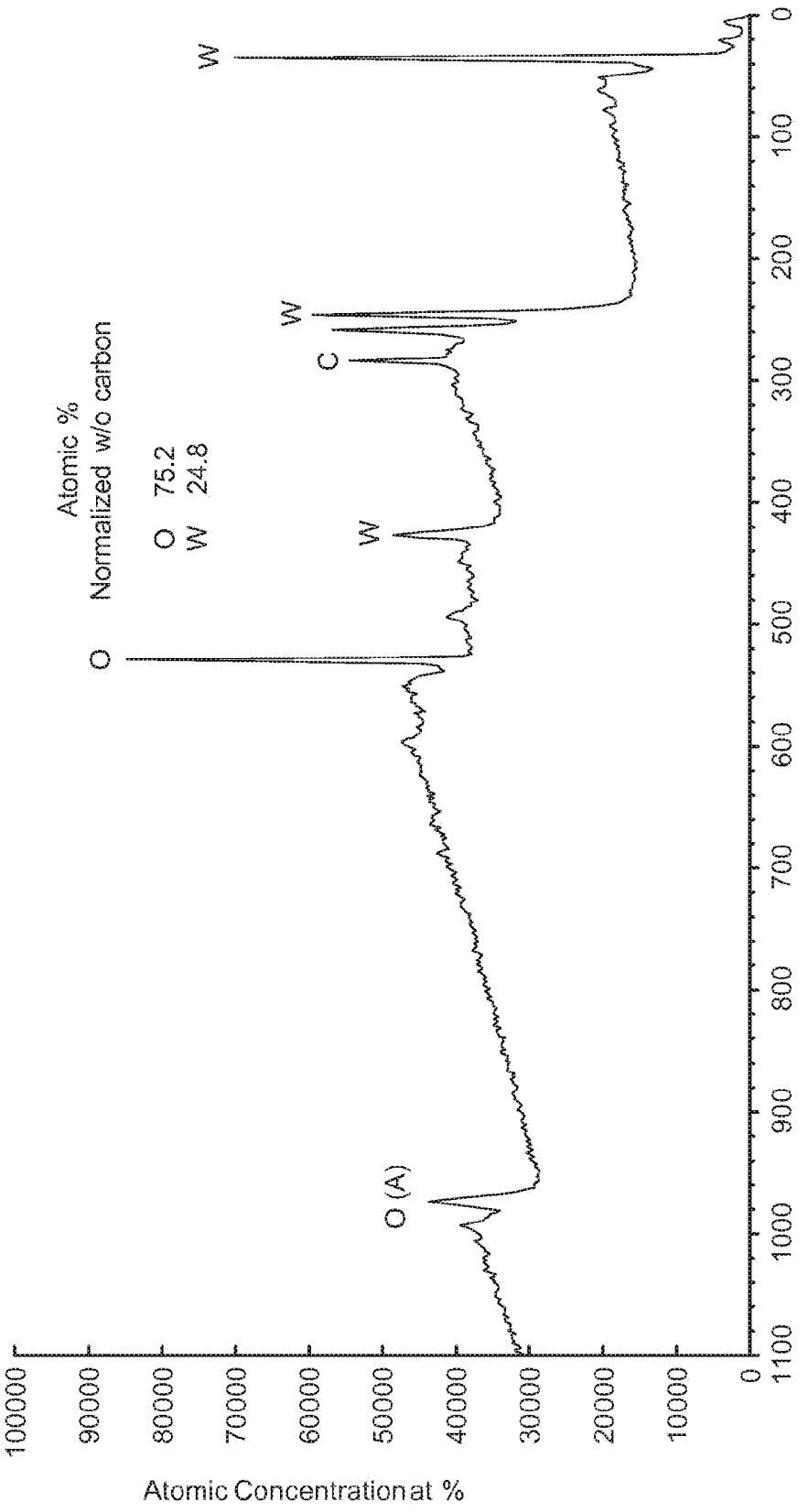
Atomic %
Normalized w/o carbon
O 75.2
W 24.8
O
O (A)
W
C
W
W
Atomic Concentration at %
B.E. eV
100000
90000
80000
70000
60000
50000
40000
30000
20000
10000
0
1100
1000
900
800
700
600
500
400
300
200
100
0

Fig. 11

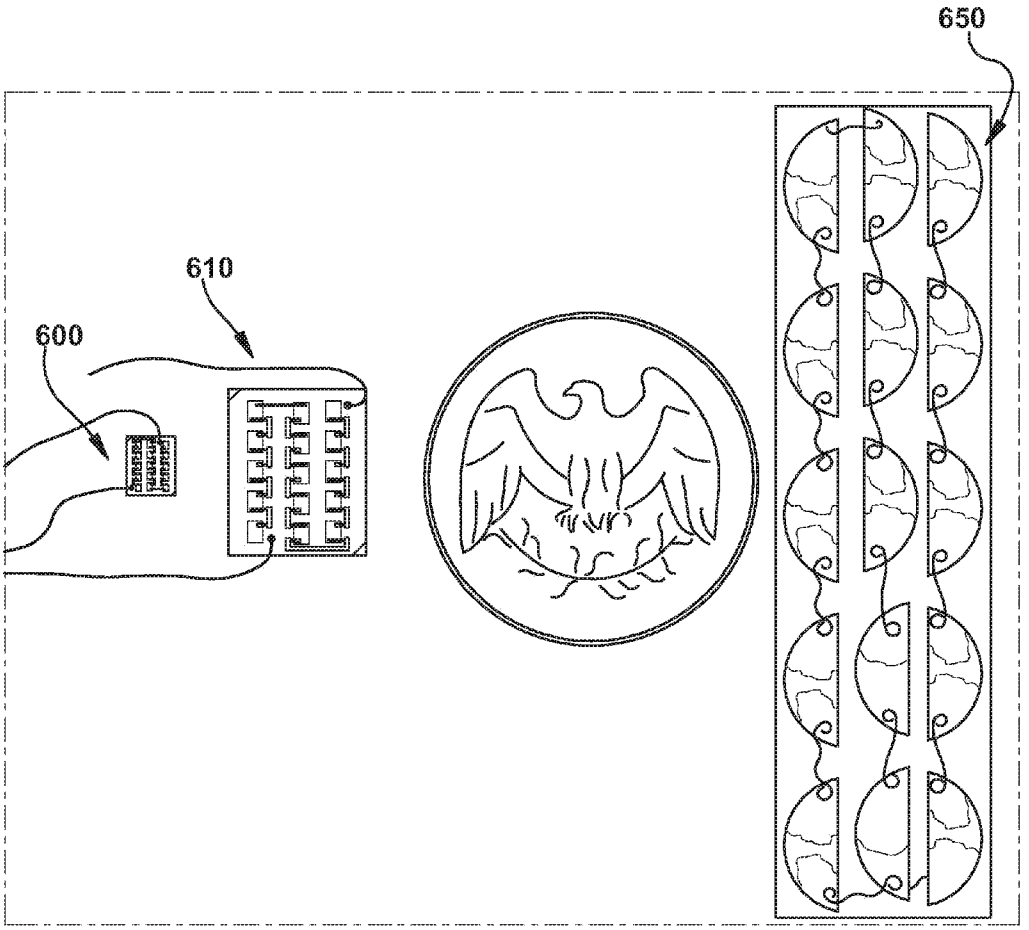

Fig. 12

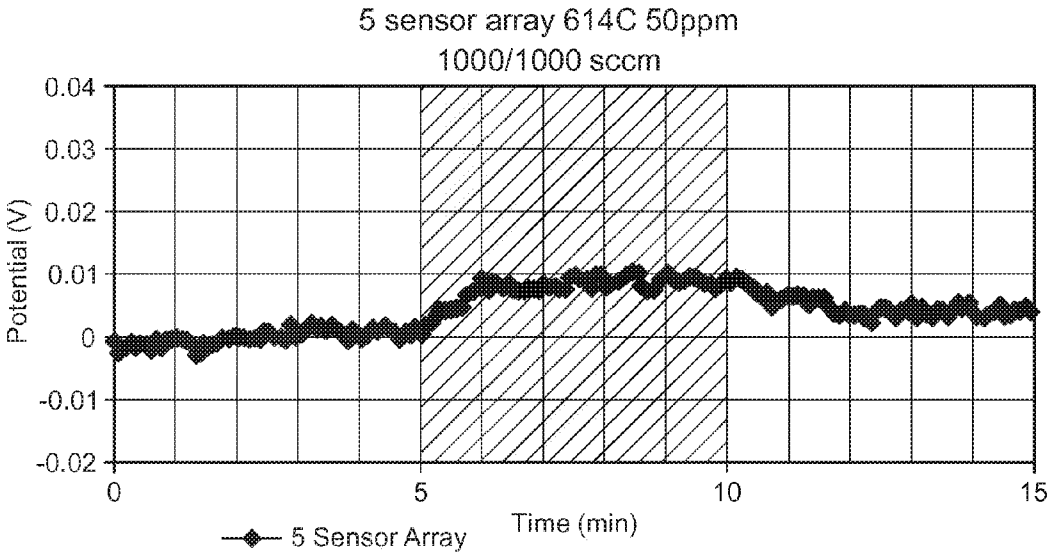
5 sensor array 614C 50ppm
1000/1000 sccm
0.04
0.03
0.02
0.01
0
-0.01
-0.02
Potential (V)
0
5
10
15
Time (min)
5 Sensor Array

Fig. 13

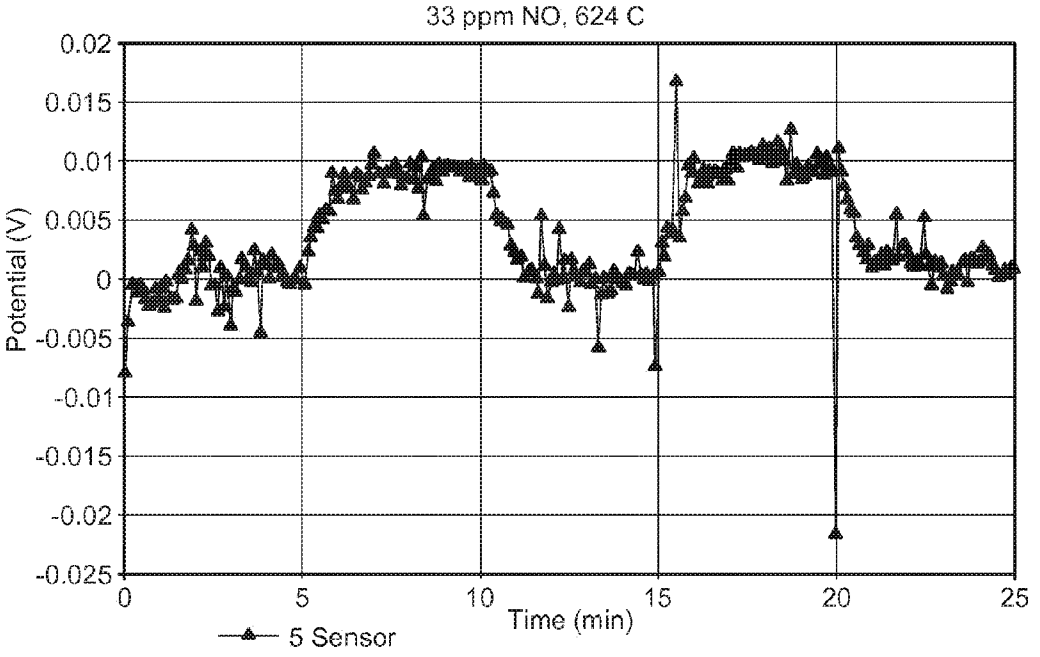
33 ppm NO, 624 C
0.02
0.015
0.01
0.005
0
-0.005
-0.01
-0.015
-0.02
-0.025
Potential (V)
0
5
10
15
20
25
Time (min)
5 Sensor

Fig. 14

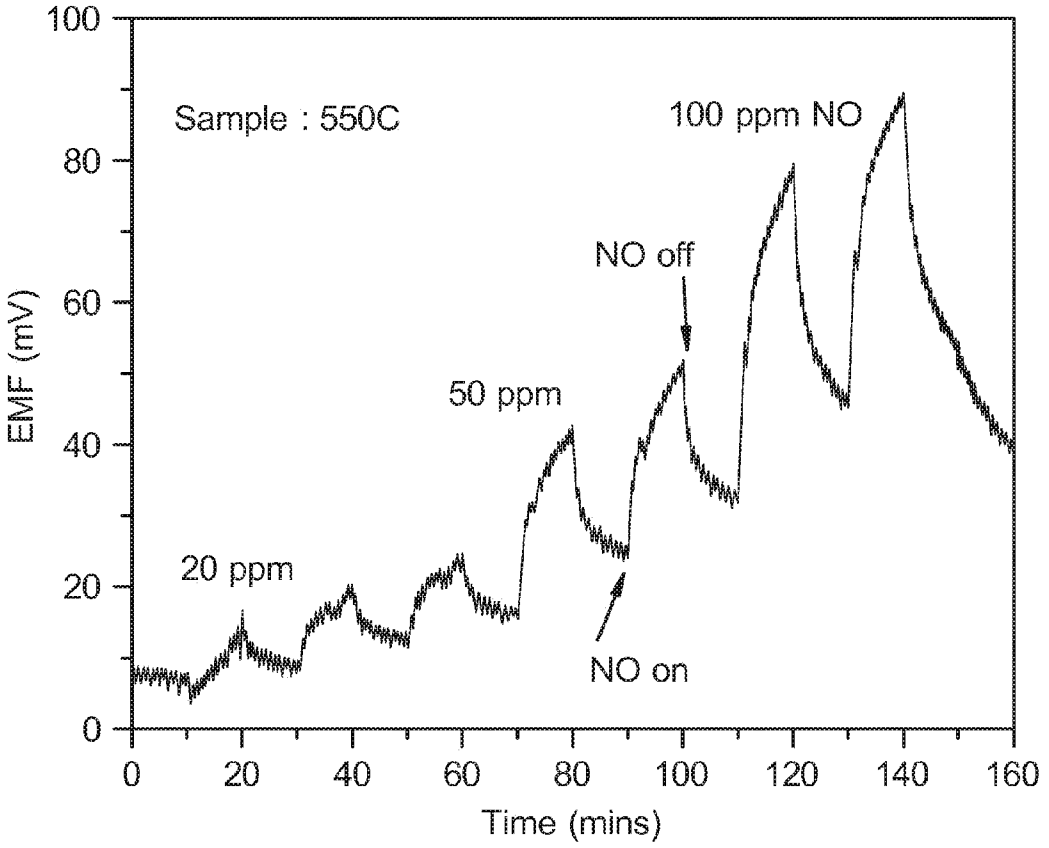
Sample : 550C
100 ppm NO
NO off
50 ppm
20 ppm
NO on
EMF (mV)
Time (mins)
0
20
40
60
80
100
120
140
160

Fig. 15

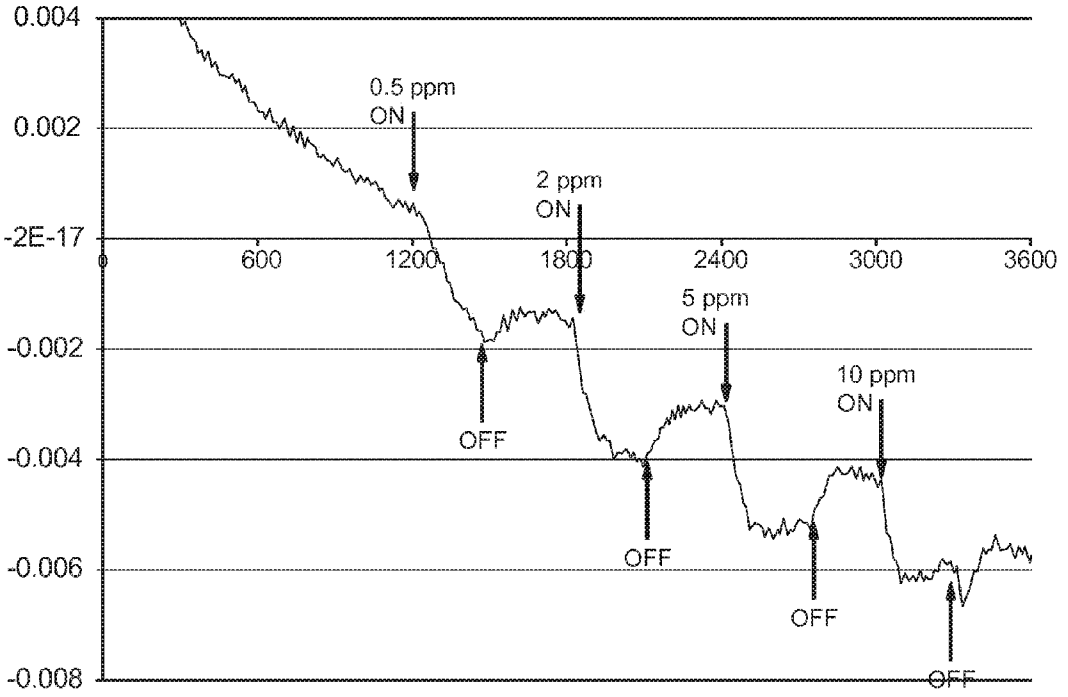
0.004
0.002
-2E-17
-0.002
-0.004
-0.006
-0.008
0
600
1200
1800
2400
3000
3600
0.5 ppm
ON
2 ppm
ON
5 ppm
ON
10 ppm
ON
OFF
OFF
OFF
OFF

Fig. 16

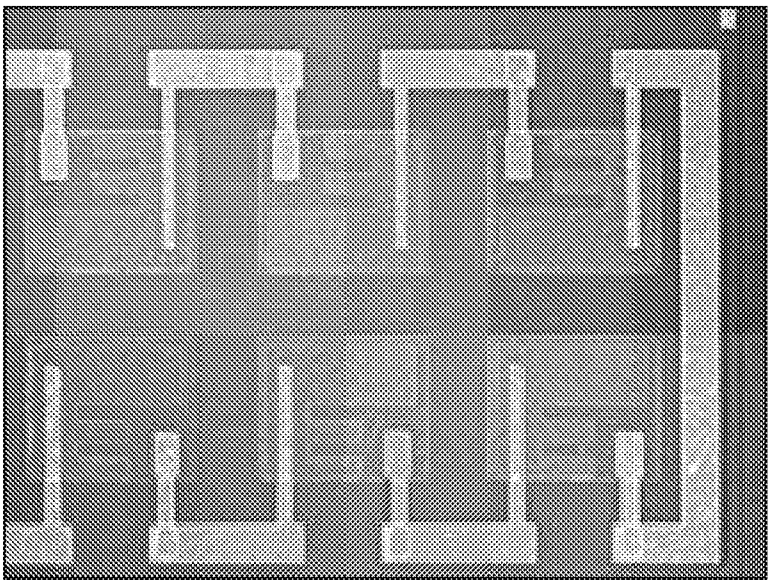

Fig. 17

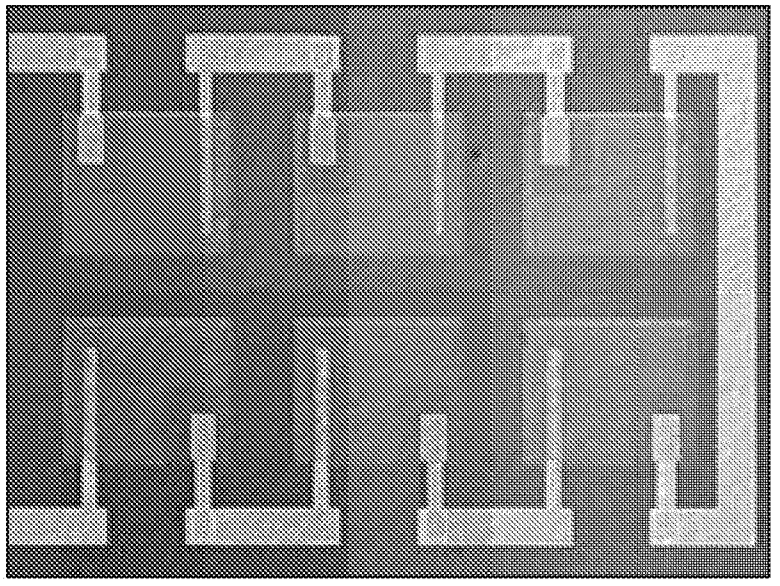

Fig. 18

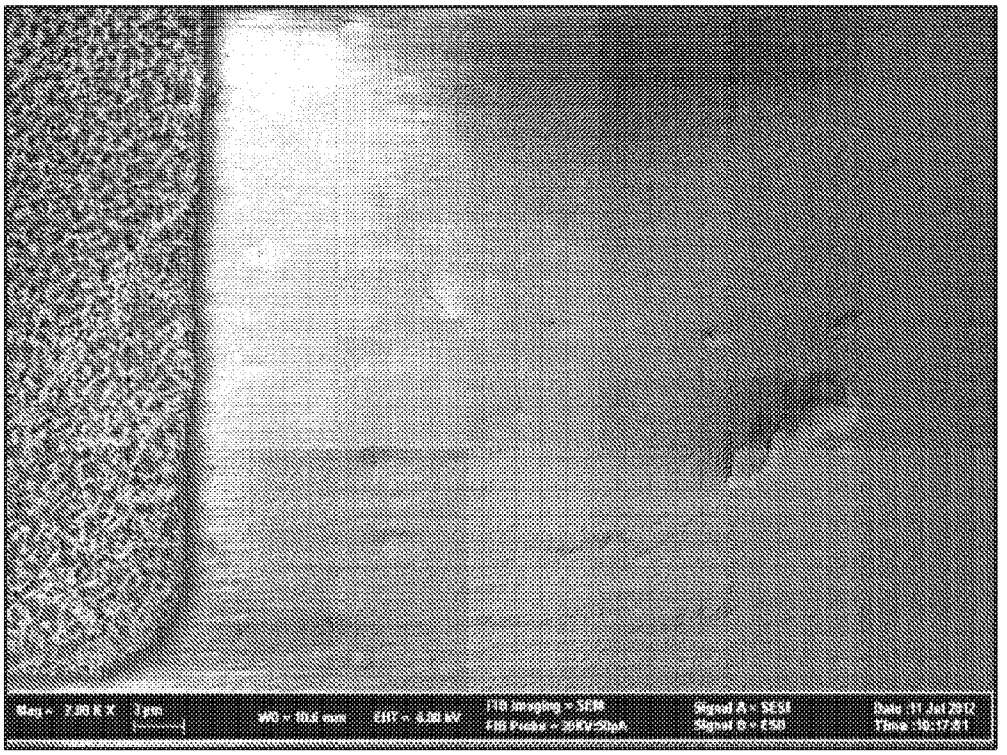

Fig. 19a

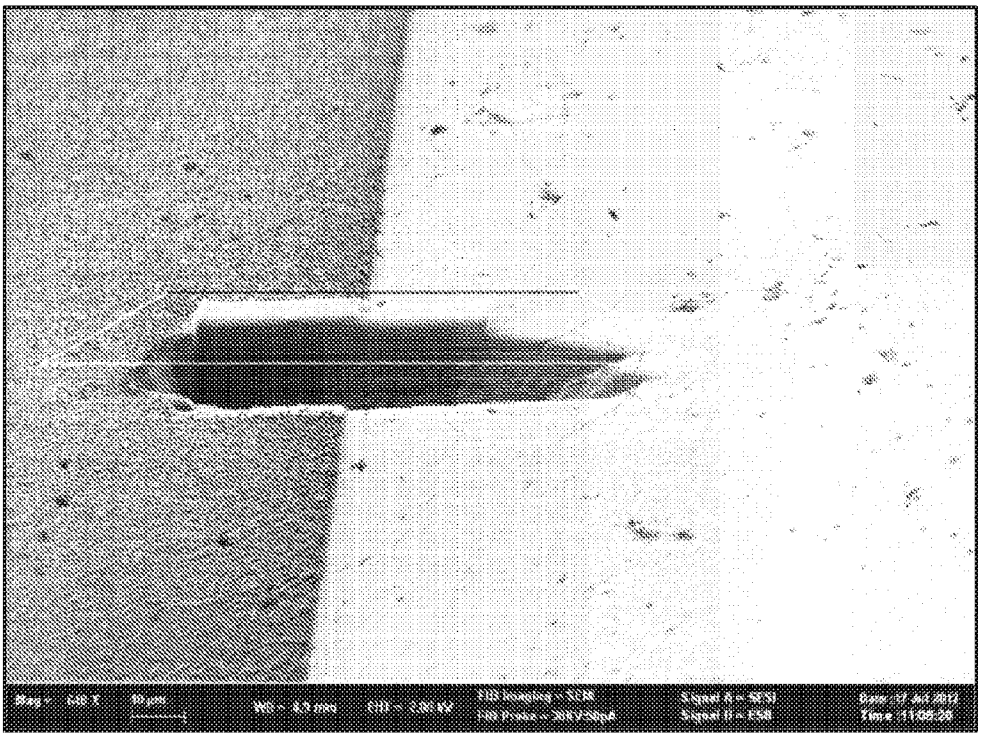

Fig. 19b

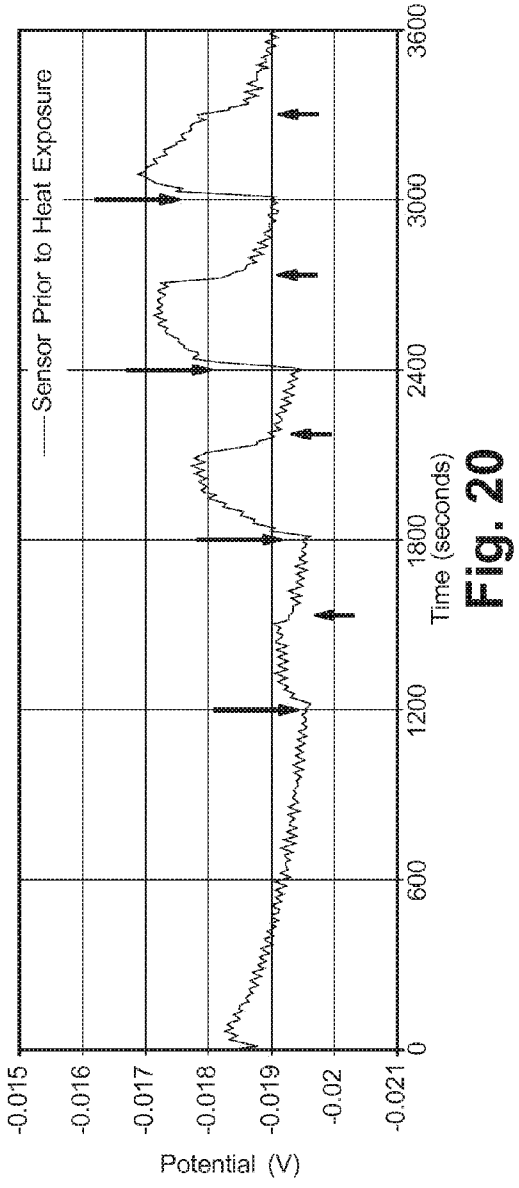
Sensor Prior to Heat Exposure
-0.015
-0.016
-0.017
-0.018
-0.019
-0.02
-0.021
Potential (V)
0
600
1200
1800
2400
3000
3600
Time (seconds)

Fig. 20

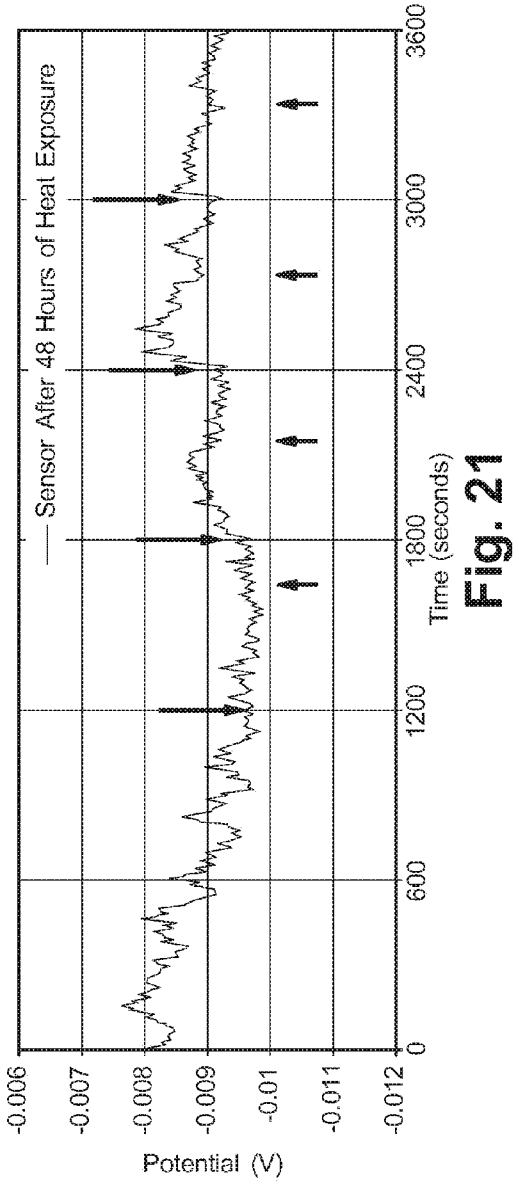
Sensor After 48 Hours of Heat Exposure
-0.006
-0.007
-0.008
-0.009
-0.01
-0.011
-0.012
Potential (V)
0
600
1200
1800
2400
3000
3600
Time (seconds)

Fig. 21

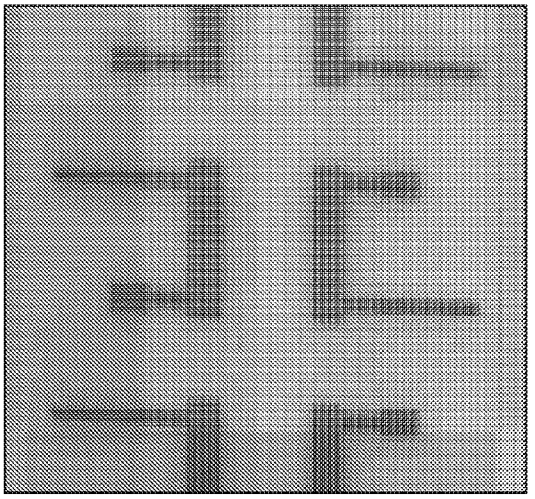

Fig. 22

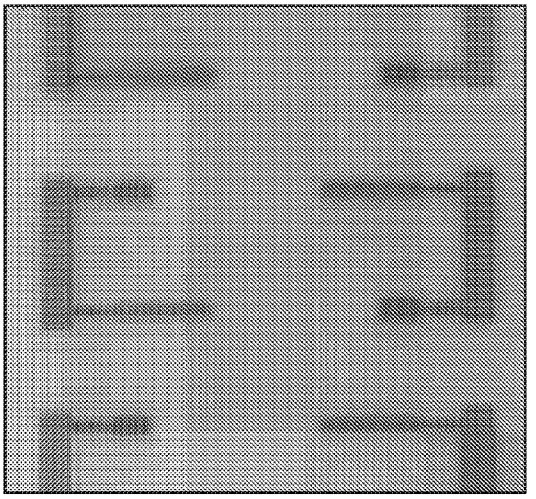

Fig. 23

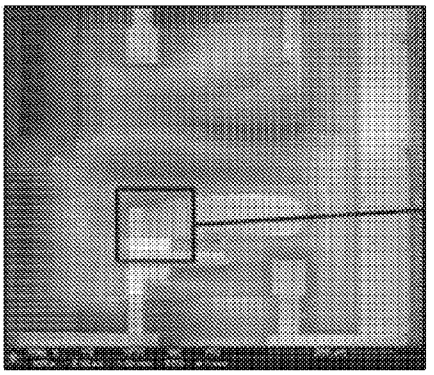

Fig. 24a

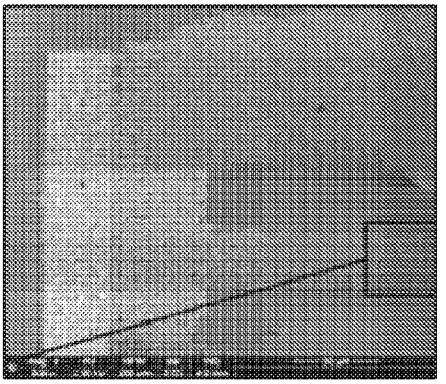

Fig. 24b

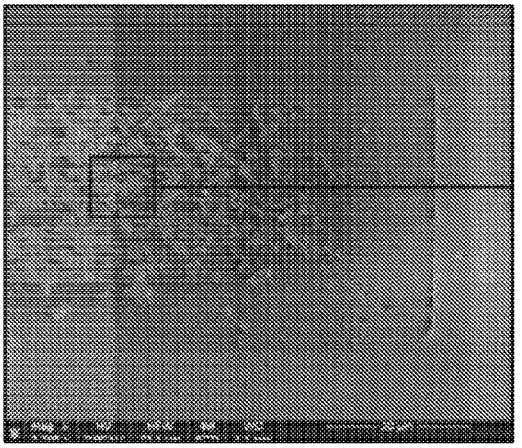

Fig. 24c

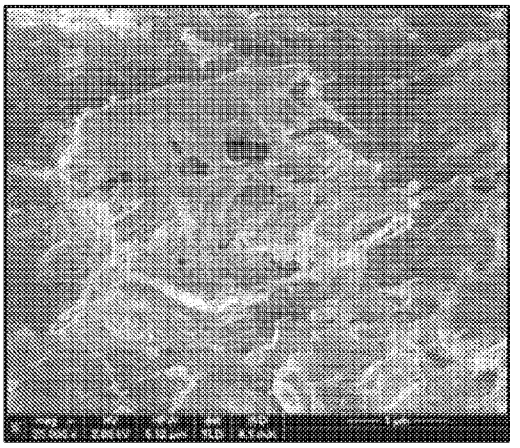

Fig. 24d

MINIATURIZED GAS SENSOR DEVICE AND METHOD

RELATED APPLICATION

This patent application claims priority to Application Ser. No. 61/801,106 entitled "Miniaturized Gas Sensor and Method" filed on Mar. 15, 2013, the entirety of which is incorporated by reference herein.

TECHNICAL FIELD

The embodiments of the present invention relate generally to gas sensors. More specifically, the disclosure relates to miniaturized gas sensors that detect NO_x gas.

BACKGROUND OF THE INVENTION

Nitric oxide (NO) sensing is a critical capability for a variety of applications ranging from high temperature combustion to clinical analysis. In high temperature combustion applications, detection of nitrogen oxides (NO_x) is critical in controlling the processes used to reduce the NO_x emissions produced by the leaner combustion processes being developed to improve fuel efficiency. NO_x sensors that are high temperature capable may also find use in other high-temperature applications. Another area where NO_x sensing is required is in the medical industry, specifically in breath analysis. These do not typically involve applications where the sensor operates in a high temperature ambient environment, but it is one where the detection of nitric oxide (NO) itself has high importance.

There are a variety of ways to detect NO, with solid-state electrochemical sensors being one such technique. Such sensors also have the added benefit of being easier to miniaturize compared to other techniques. A variety of solid-state electrochemical sensors for NO have been demonstrated previously. These techniques vary and a continuing challenge is to design sensitive systems with limited size, weight and power consumption so as to allow for portable sensor systems. Such advancements would have notable impact on the healthcare industry in enabling home-care monitoring units.

NO sensors capable of detecting NO at concentrations as low as 7 ppb have been demonstrated using an array of sensor units in series to increase the resulting sensor signal for a given NO concentration. However, these sensors were made using hand assembly techniques and also were assembled into arrays by hand. This manual fabrication limits the minimum size to which the sensors can be reduced.

Miniaturized sensors based on microelectromechanical systems (MEMS) fabrication technology have been demonstrated for aerospace applications. Sensors made by MEMS fabrication are very small devices that can be made up of components and features between 1 to 100 micrometers in size (0.001 to 0.1 mm). Fabrication is a challenge at these size scales for several reasons. Large surface area to volume ratio of MEMS, and the resulting surface effects which dominate over volume effects can improve sensor performance. However, the overall surface area of a MEMS sensor unit may be notably smaller than corresponding macro sensor devices. This may decrease the overall number of chemical reactions involved, resulting in a decreased signal. Thus, improved sensor design is mandatory to enable miniaturization of sensor systems. Such optimization may be different on the macro level then for micro sensors, and

simple application of design principle that are successful for macro sensor can lead to significantly degraded performance for micro sensors.

A reduction in size of the sensors using MEMS techniques would not only decrease the size for better implementation in a handheld home monitoring unit, but the reduced size would also decrease the power required to bring the sensors up to operating temperature. In addition, the utilization of MEMS fabrication techniques introduces batch fabrication that allows for multiple sensors to be made at one time, thus reducing costs.

SUMMARY

Various embodiments of a microfabricated gas sensor device and method of fabricating a miniaturized gas sensor device are provided. In one embodiment a microfabricated gas sensor device includes a base substrate, an electrolyte layer disposed on the base substrate and a plurality of potentiometric sensor units electrically coupled together on the base substrate. Each potentiometric sensor unit includes an electrolyte layer disposed on the base substrate, a sensing electrode comprising tungsten oxide (WO_3), a reference electrode comprising platinum (Pt), and a plurality of connectors coupled to the plurality of potentiometric sensors to connect the plurality of potentiometric sensors in series. The structure of each of these potentiometric sensor units is designed to greatly improve sensor response.

BRIEF DESCRIPTION OF THE DRAWINGS

The example embodiments of the present invention can be understood with reference to the following drawings. The components in the drawings are not necessarily to scale. Also, in the drawings, like reference numerals designate corresponding parts throughout the several views.

FIG. **1** illustrates a miniature sensor device, which is a first generation design using shadow masks, according to an embodiment of the present invention;

FIG. **2** illustrates a miniature sensor device, which is a second generation design using shadow mask, according to an embodiment of the present invention;

FIGS. **3***a*-**3***b* illustrate an alumina substrate used for sensor fabrication;

FIGS. **4***a*-**4***b* illustrate the deposition of YSZ islands during sensor fabrication;

FIGS. **5***a*-**5***b* illustrate the deposition of the Pt electrodes during sensor fabrication;

FIGS. **6***a*-**6***b* illustrate the deposition of WO_3 during sensor fabrication;

FIG. **7** is a flow chart of the method for making the sensor device, according to an embodiment of the present invention;

FIG. **8** illustrates a photographic image taken under a microscope of one of the sensor units in the first generation, shadow mask design of FIG. **1**, according to an embodiment of the present invention;

FIG. **9** illustrates a photographic image taken under a microscope of a sensor unit of the second generation, shadow mask design of FIG. **2**, according to an embodiment of the present invention;

FIG. **10** illustrates a photographic image taken under a microscope of an alternative miniature sensor unit of a second generation, shadow mask design, according to an embodiment of the present invention;

FIG. **11** illustrates the spectrum from XPS analysis of sputter deposited WO_3 film, in accordance with an embodiment of the present invention;

FIG. **12** illustrates a miniature sensors of the second generation shadow mask design, and a photoresist version of the miniature sensor compared to a hand fabricated sensor, according to an embodiment of the present invention;

FIG. **13** illustrates the test results of a miniature five sensor unit device of the first generation, shadow mask sensor design at 50 ppm exposure to NO, according to an embodiment of the present invention;

FIG. **14** illustrates the test results of a miniature five sensor unit device of a second generation, shadow mask sensor design at 33 ppm exposure to NO, according to an embodiment of the present invention;

FIG. **15** illustrates test results of a miniature ten sensor unit device of a second generation, shadow mask design in a plot of sensor voltage response to 20 ppm, 50 ppm, and 100 ppm NO exposure, according to an embodiment of the present invention;

FIG. **16** illustrates the test results of a miniature fifteen sensor unit device of a second generation, photolithographic design in a plot of sensor response to 0.5 ppm, 2 ppm, 5 ppm, and 10 ppm NO exposure, according to an embodiment of the present invention;

FIG. **17** illustrates a photographic image showing a six sensor unit device of a second generation, photolithographic design, according to an embodiment of the present invention;

FIG. **18** illustrates a photographic image showing a six sensor unit device of an alternative second generation, photolithographic design, according to an embodiment of the present invention;

FIGS. **19***a* and **19***b* are SEM images of sensor showing cracks of the YSZ following the photolithographic process, according to an embodiment of the present invention;

FIG. **20** illustrates a plot of test results of a sensor device before extended heat exposure, according to an embodiment of the present invention;

FIG. **21** illustrates a plot of test results after 48 hours of continuous heat exposure, according to an embodiment of the present invention;

FIGS. **22** and **23** before and after, respectively, extended heat exposure, according to an embodiment of the present invention; and

FIGS. **24** *a-d* illustrate SEM images of sensor region containing WO3 after heat exposure, according to an embodiment of the present invention.

DETAILED DESCRIPTION

The various embodiments of miniature NO sensors disclosed herein is an electrochemical sensor whose structure includes sensor units of solid electrolyte, a reference electrode and a working electrode. An electromotive force (EMF) is induced between the working and reference electrodes when NO impinges on the sensor due to the dissimilar chemical activity at each electrode. In one embodiment, the reference electrode is platinum (Pt), while the sensing or working electrode is tungsten oxide (WO_3). The solid electrolyte is yttria-stabilized zirconia (YSZ). These sensor material choices are based on larger hand-made sensors that are described further in the examples below.

FIG. **1** shows a miniature sensor device **10** having individual sensor units **50** and fabricated on aluminum oxide substrates **12**. Each sensor on the substrate comprises a YSZ island **50** upon which the rest of the sensor is built. Pt reference electrode **52** and WO_3 sensing or working electrode **54** lie on top of the YSZ island **51**. A Pt contact **55** of the sensing electrode is located below the WO_3 to make contact to the WO_3 of this two-part sensing or working electrode. As each sensor **50** is an electrochemical cell, the sensors can be connected in series to generate a larger signal response. Thus, an array of sensors can be used to improve the signal response to NOx, including NO. The sensors are electrically connected together as in the cells of a battery such that the induced EMF's are additive, thereby increasing the response for a given NOx concentration over a single sensor. Sensor devices of 5, 10, 15 and 20 sensors were connected electrically and tested. Each sensor array is interconnected electrically via Pt leads. This fabrication approach represents a simple reduction in size of the larger in the sensors and it has been found herein, as demonstrated in the examples below, that simple reduction in size does not result in the desired sensitivity needed to improve sensor performance.

With reference to FIG. **1**, the gas sensor device **10** includes a plurality of, i.e. or at least two, sensor units **50** in a dice unit row **12**. Each of the sensor units **50** includes a reference electrode **52** and a sensing electrode **54**. In one embodiment, the sensing electrodes **54** comprise WO_3, and the reference electrodes **52** comprise platinum (Pt).

In one embodiment, the gas sensor device **10** includes 3 rows **14** of sensor units **14**, but a variety of sensor units **50** is possible. Each of the sensor units **50** is electrically coupled to at least one adjacent sensor unit **50**. For example, the sensor units **50** are electrically connected together in series. The combined potential difference of the plurality of sensor units **50** is approximately a sum of the potential differences of each of the individual sensor units **50** electrically connected to one another.

Experimental tests that have been conducted herein show that the sensitivity of the system **10** is based on the number of sensor units **50**. Each of the sensor units generates a potential difference in the response to a gas, for example, NO_x gas. Generally, a system including more sensor units **50** has been found to be relatively more sensitive to NO, and a system including less sensor units has been found to be relatively less sensitive to NO. However, there is a point at which additional sensor units **50** will not improve the sensitivity, and it has been found that sensor devices that have 15-20 sensor units have increased sensitivity. This is due to lack of previous recognition of the various elements of sensor design including, for example, the internal resistance of each sensor element. As noted above, a corresponding reduction of the size of the sensor having the same materials of construction do not result in improved sensitivity. The impact of the internal resistance of the individual sensor units, and the design features that contributed to higher sensitivity is described herein and was discovered during the course of the fabrication of sensors as discussed in the examples below. Overcoming internal resistance is core to even higher levels of sensitivity.

It has been found herein, in accordance with various embodiments of the present invention, that reducing the exposed surface area of Pt reference electrode on the YSZ electrolyte and increasing the surface area of WO_3 electrode covering the YSZ electrolyte improves the sensitivity of the sensor as can be seen in comparing the results of the first generation, shadow mask design of FIG. **1** and second generation, shadow mask design of FIG. **2** and shown in the results of the examples. FIG. **2** shows a miniature sensor device having individual sensor units **60** and fabricated on a substrate, for example, aluminum oxide substrates. Each

sensor on the substrate comprises a YSZ island **50** upon which the rest of the sensor is built. Pt reference electrode **62** and WO_3 sensing or working electrode **64** lie on top of the YSZ island **61**. A Pt contact **65** of the sensing electrode is located below the WO_3 to make contact to the WO_3 of this two-part sensing or working electrode. As each sensor unit **60** is an electrochemical cell, the sensors can be connected in series as a sensor device to generate a larger signal response. Thus, an array of sensors can be used to improve the signal response to NO.

The ratio of the exposed WO_3 to the exposed platinum Pt is maximized to increase the sensitivity and obtain a low end sensor reading. Furthermore, in another embodiment, the ratio of the exposed WO_3 to the exposed platinum Pt is maximized while also decreasing the size, for example the surface area, of the Pt contact of the sensing electrode that is contact with WO_3. Decreasing the size of the contact **65** underneath the WO_3 so that it is minimized to the extent of fabrication (i.e. within the resolution of the fabrication approach, such as 2 microns) is found to increases the sensitivity of the microfabricated sensors units **60**. This electrode structure is not a simple one component electrode, but rather composed of both an oxide and metallic electrode combination that together are designed for improved response. In accordance with an embodiment of the present invention, the electrolyte layer of the microfabricated potentiometric gas sensor device has a thickness of the electrolyte layer that is maximized a sufficient amount to minimize the internal resistance of the potentiometric sensor unit, and such that the internal resistance of each of the plurality of sensor units is minimized so as to minimize the overall resistance of the sensor device to increase the sensitivity of the sensor device.

For example, in one embodiment the surface area of the WO_3 electrode on the electrolyte is greater than the surface area of the Pt electrode. In another embodiment the WO_3 covers all of the available surface on the YSZ unused by the Pt electrode within the resolution of the fabrication approach (approximately 2 microns depending on the equipment used). In another embodiment the surface area of the WO_3 electrode is at least two times greater than the surface area of the Pt electrode, and in another embodiment, the WO_3 electrode is at least 5 times greater than the surface area of the Pt electrode, and in yet another embodiment the WO_3 electrode is at least 10 times greater than the surface area of the Pt electrode.

The increased surface area of the WO_3 boundaries does increase the triple point boundary of the WO_3 electrode, the YSZ electrolyte and the gas, for example, NO gas compared to those of the Pt electrode. The decreased surface area of the Pt electrode decreases the triple point boundary of the Pt, the YSZ electrolyte and the gas. The limitation on the amount of YSZ surface area that is not also a triple point boundary is believed to decrease the sensitivity of the sensor. As a result it has been found that the sensitivity of the sensor device can be increased.

In addition FIG. **9** shows that the surface of the WO_3 electrode **310** of sensor unit **300** has at least one lateral projection **320**. The at least one lateral projection has at least two edge interfaces **330**, **340** along the surface of the electrolyte, and in another embodiment at least three edge interfaces, thereby creating additional triple point boundary points between the WO_3 electrode and YSZ electrolyte. In another embodiment, FIG. **10** shows that the surface of the WO_3 electrode has three lateral projections **420**, **430** and **440**. Each lateral projection has at least three edge interfaces **510**, **520** and **530** along the surface of the electrolyte which forms a triple point boundary between the WO_3, the YSZ electrolyte and the gas. As shown the lateral projections form corners formed by the edge interfaces **520** and **530**. These lateral projections increased the torturous nature of the pattern and increase the number of triple points. For example, these lateral surface contours increase the lineal length of edge interface between the WO_3, the electrolyte, and the surrounding gas as illustrated in FIGS. **9** and **10**.

Further, the size of the YSZ patterns in FIG. **2** compared to FIG. **1** decreases the distance, and thus corresponding resistance, between the electrodes. Other factors decreasing this resistance include the thickness of the electrolyte, yttria-stabilized-zirconia, and thickness of the various metal layers that are micro-deposited on the surface. Such features are not apparent in macro sensor since, for example, a 5 micron change in the thickness of the zirconia in a macro sensor has much less effect on the internal resistance of the sensor unit where it would nearly eliminate the zirconia layer for a microfabricated sensor.

It should be noted that this is a potentiometric sensor (voltage difference), rather than an amperometric sensor (current flow). In a sensor that measures current flow, the effect of resistance is known and too large a resistance can readily be seen to limit the measurement. Such amperometric sensors are not linked in series like batteries (as are the potentiometric sensors in our work) and the effect of increase resistance is directly noticeable in the measurement. It is discovered that an aspect of the potentiometric sensor device that includes sensor units linked in series, is that high resistance of each sensor unit was found to limit the lower detection limit of the sensor overall. Thus, while each sensor unit might have a resistance that did not notably affect its operation; the combined resistance of each of the potentiometric sensor unit in series can change the lower limit detection capabilities of the overall sensor. This may not be obvious at higher concentrations, but was found to have significant effect on sensitivity for lower concentration measurements. It was found that decreasing this overall resistance is a feature of increasing the sensor's lower detection limit.

The microfabricated potentiometric gas sensor device senses gas at a broad range of temperatures, including but not limited to, high temperatures that range from about 500° C. to about 700° C., in another embodiment, from about 550° C. to about 650° C.

Method of Fabrication

MEMS fabrication has been successfully implemented in the examples herein, where sensors are batch fabricated on a single wafer, with each wafer containing multiple sensors units. These examples show that applying the concepts above are not only achievable but improve the capability of the sensor. These examples are meant to show different aspects of the design optimization from large to smaller sensors and so while one example may show improved response time but decreased response, it is the combination of the various design features that is understood to provide an improved sensor system, or may be used as needed to emphasize certain aspects of the sensor response. The sensors are fabricated using masks and thin film deposition techniques. Each layer of the structure is deposited via sputtering from a target containing the desired material or a component of the desired material, with the masks serving to define the shape of the resulting deposited film. The fabrication of these sensors was carried out using thin metal, shadow masks or photoresist masks. The sensors were fabricated on two-inch alumina wafers.

The general process flow for the sensors is shown in FIG. **7**. The first step in the fabrication process is to clean the alumina wafer using a combination of solvents, generally acetone followed by isopropanol. The YSZ islands are sputter deposited using the first mask, forming individual rectangular islands of YSZ. A thermal anneal is then carried out at 1000° C. for two hours in air ambient to densify the YSZ. The Pt electrodes are then deposited using the next mask. A second platinum layer is sputter deposited to form the interconnects, electrically connecting the sensors in the array. It should be noted that in some designs of the sensor device the Pt interconnects are deposited at the same time as the first Pt electrode deposition. Finally, the WO_3 is reactively sputter deposited from a tungsten target in an argon/oxygen atmosphere using the third mask. The sensors are then diced into individual arrays following the final film deposition.

The three films that are deposited are the YSZ, Pt, and WO_3 films. Both the YSZ and Pt films are deposited by a sputter deposition process. The WO3 also is deposited by a sputter process. However, the sputter process is a reactive sputter process using a tungsten (W) target whereby a W target is sputtered to produce W atoms that are then reacted with an oxygen gas flow in the chamber prior to impingement on the substrate where they are deposited as WO_3. The deposition is done at room temperature using a cooled substrate to keep the substrate cool. XPS analysis on the films confirmed the proper stoichiometry of the films after the sputter deposition processes, as shown in FIG. **10**. No sensors fabricated using thin film microfabrication techniques that are significantly smaller than such sensors are herein demonstrated. Changes made from the initial design to the size of both the reference and working electrode as well as the contacting Pt electrode under the working electrode resulted in improved sensitivity of the sensor. These sensors have demonstrated sensitivity below the ppm level.

FIGS. **3** through **6** illustrate a sensor array at various steps of a fabrication process, according to an embodiment of the present invention. Cross-sectional and top views are shown left and right, respectively: (a) Alumina substrate, (b) deposition of YSZ islands, (c) following deposition of Pt electrodes, (d) sensor after deposition of WO_3, according to an embodiment of the present invention;

FIGS. **3**A and **3**B show the base layer of alumina used in the substrate **100** in an embodiment of the present invention. FIGS. **4**A and **4**B show a side view and top view, respectively, of the alumina substrate **100** with an electrolyte layer **102** deposited on the substrate. FIGS. **5**A and **5**B show a side view and top view, respectively, of the substrate **100** with the electrodes **104** deposited on top of the electrolyte layer **102**. FIGS. **6**A and **6**B show the side view and top view of the tungsten oxide WO_3 electrode **106** which is the working electrode deposited on top of the Pt contact **104**.

FIG. **7** illustrates the process step for making the gas sensor. In one embodiment the box **205** shows the first step of cleaning the alumina wafer substrate. Solvents or combinations of solvents, for example alcohols acetone and isopropanol, or an application of solvent in a series of acetone followed by isopropanol can be used to clean the substrate. In box **210** the mask is placed on the substrate, a thin metal mask for the shadow mask design and a photoresist mask in the photoresist design n box **210**, for the photoresist design the photo resist mask is applied to the surface of the substrate. Once the photoresist mask is deposited, the substrate is soft baked to remove some of the solvents in the liquid photoresist. Then the photoresist is placed under a UV light source and the UV light is selectively passed through a glass mask with defined openings through which light may pass to the photoresist. Depending on whether the photo resist is positive or negative, the resulting regions exposed to light will either become more soluble or less soluble respectively after exposure to the UV light. The substrate is then placed into a developing solution that removes the more soluble regions of the photo resist. The substrate is then placed under heat for a hard bake of the photo resist mask. In the next step of box **215** the process includes depositing a layer of electrolyte using a sputter deposition of the desired film. The photo resist is then removed by a solvent, usually acetone, and the sputtered film on top of the photo resist is also removed leaving behind the thin film that was defined by the openings in the photo resist mask. The photo resist mask has precisely defined features down to below 100 micrometers which is a much smaller resolution than the shadow mask used in the embodiments described above. Next in box **220** the substrates were annealed in the presence of oxygen in order to remove or clean the residual photo resist from the surface. It was found that standard techniques to remove the photo resist perform poorly and the miniaturization process did not provide good results compared to the shadow mask method of making the sensor when using the standard software-based photoresist removal techniques. The oxygen annealing temperature to remove the residual photo resist on the surface or in the pores of the films of the sensor can be carried out at a temperature that is at least 350° C., and another embodiment from about 350° C. to about 450° C., and in another embodiment from about 390° C. to 425° C. It has been found that residual photoresist can notably affect sensor response and the oxygen annealing step, in accordance to an embodiment of the present invention was found to improve sensitivity.

Still referring to FIG. **7**, the process for making the gas sensor further includes applying another mask over the electrolyte layers and next in box **230** the process further includes depositing the reference electrode material and contact material for the sense electrode over the mask but through sputtering. The mask is removed and for the photoresist-based sensor the substrate is again annealed to remove residual mask material in box **235**. Next in box **240** another mask is again applied over the substrate and over the electrodes to deposit the connectors in box **250**. In another embodiment the reference electrode, contact for the sense electrode, and the connectors can be applied in a single step after application of the mask in box **210**. Next in box **260** the mask is removed and for the photoresist-based sensor the substrate then undergoes the annealing process to remove the residual photoresist. Next in box **265** the mask is applied again and then in box **270** the sensing electrode is deposited by reactive sputtering. Next the mask is removed and for the photoresist-based sensor the substrate undergoes another annealing process as shown in box **270** to remove all residual photoresist. Finally, in box **280** the substrate can undergo dicing to separate the individual sensor arrays **10** on the substrate. The oxygen annealing temperatures of boxes **235**, **260**, and **275** are carried out and are the same as the temperature ranges described above with respect to box **220**.

The results of the testing on these various generations of designs indicate that the changes that were made between each generation were indeed beneficial to the overall performance of the sensor. Reducing the exposed Pt on the YSZ and increasing the WO3 covering the YSZ improved the sensitivity of the sensor as can be seen in comparing the results of the first and second generation shadow mask

designs. The resulting design changes were applied to the photomask-based design, which is basically the second generation shadow mask design reduced in size by a factor of 0.35. The test results of the photoresist design indicate that the sensor array should be capable of sensing down to at least 500 ppb level, and in another embodiment down to about 300 ppb level.

In another embodiment, the several embodiments of the NO sensor device described above can be used in an apparatus for measuring the level of NO. The apparatus includes the sensor device and an inlet for receiving a gas sample. The gas sample, for example, NO gas, is in fluid communication with the sensor. The potential difference is indicative of a level of NO within the original sample. In one embodiment, the gas sample is a breath sample from the subject. In another embodiment, the gas sample that enters the apparatus may be treated by humidification or dehumidification to improve the sensitivity. The potential difference of the sensor array **10** is a summation of the individual potential differences across the individual sensor units in response to presence of the NO in the gas sample.

EXAMPLES

Examples—Shadow Mask Fabrication

The shadow mask version of the sensor arrays utilized a metal shadow mask during each of the deposition processes to define the deposited films into the desired features. The metal masks were placed onto the substrate and clamped at the edges of the substrate. The shadow masks are easy to use and are aligned from one mask layer to the next. However, the defined features are rather large in size, there can be distortion in the shadow mask resulting in edges of the defined shapes that are not sharp, and after multiple uses the resulting film build up on the shadow masks may cause warpage of the shadow mask and/or micromasking during the deposition process as particles fall off of the shadow mask and land on the openings defined by the mask.

For comparison, our initial sensor design is shown in FIG. **1** with corresponding dimensions, along with the second generation, shadow mass that is illustrated in FIG. **2**. FIG. **1** shows that the electrolyte island **51** dimension A is 1.55 mm by 2.88 mm; the Pt reference electrode **52** of dimension B is 1 mm×0.21 mm; the Pt interconnect **53** of dimension C has an outer length of 1.56 mm and an inner length of 1.15 mm; the sensing electrode **54** of WO_3 has a dimension D of 1.1 mm×0.31 mm; and the Pt contact **55** of the sensing electrode E is approximately the same surface area as the reference electrode **52**. FIG. **2** shows that the electrolyte island **61** dimension N is 1.328 mm by 1.55 mm; the Pt reference electrode **62** of dimension I is 0.4 mm×0.21 mm; the Pt interconnect **63** of dimension G has dimensions of 0.33 mm×1.4 mm; the WO_3 of sensing electrode **54** has an "L" shape that can be calculated by dimensions L (0.54 mm), M (1.4 mm), O (1.22), and K (0.88); and the Pt contact **65** of the sensing electrode has dimensions H, 1.5 mm×0.1 mm.

FIG. **12** illustrates a comparison of sensors to hand fabricated sensor on the far right, with a quarter shown for size reference. The shadow mask version of the sensor is to the left of the quarter and is 10 mm by 12 mm. The photoresist version of the sensor is to the far left and is 3 mm by 4 mm in size.

In comparing the first and second generation shadow mask designs, the size of the WO_3 covering the YSZ is increased by a factor of 4.0 from 0.341 mm^2 to 1.35 mm^2 for the WO_3 on the YSZ in moving from design generation one to two. Similarly the Pt reference electrode was decreased in size by a factor of 2.5 from 0.21 mm^2 to 0.084 mm^2 in moving from design generation one to two. The size of the YSZ island for each individual sensor is 1.55 by 2.28 mm^2 for generation one and 1.328 by 1.55 mm^2 for generation two designs. These designs are shown in FIGS. **1** and **2**.

Examples—Photoresist Process

The second variation of the sensors that was fabricated was a photoresist-based version of the sensors. In this version of the sensor arrays, the deposited films are defined by photoresist layers deposited on the substrate. In the photoresist process a liquid photoresist film is spun onto the surface of the substrate. Once the photoresist is soft baked to remove some of the solvents in the liquid photoresist, the substrate is placed under a UV light source that is defined by a glass mask. A thin metal film on the glass mask defines openings through which light may pass to the substrate. Depending on whether the photoresist is positive or negative, the resulting regions exposed to light will either become more soluble or less soluble, respectively, after exposure to the UV light. The substrate is then placed into a developer solution that removes the more soluble regions of the photoresist. After a hard bake the photoresist mask is ready to be used as the mask for sputter deposition of the desired film. Once the sputter deposition process is finished the sputtered film is defined by a lift-off process whereby the photoresist is removed by a solvent, usually acetone, and the sputtered film on top of the photoresist is also removed leaving behind the thin film that was defined by the openings in the photoresist mask.

The advantage of the photoresist mask versus the shadow mask is that the photoresist mask can define features to a much smaller resolution (e.g., down to about 2 micrometers). The photoresist version of the sensor was decreased to 0.35 times the size of the second generation shadow mask version, the sensors are otherwise identical in layout design. The downside to the photoresist mask is the possible contamination of the underlying materials with photoresist if they are porous. If the photoresist is not completely removed following the thin film deposition the resulting remnants may react at higher temperatures and form a barrier to gas reaction at the surfaces of the sensor. In fact, sensors that were initially fabricated using standard photoresist development and removal techniques performed poorly compared to the shadow mask versions. This link between photoresist contamination and degraded sensor performance was confirmed when shadow mask versions of the sensors that were covered with photoresist prior to dicing into individual arrays by the dicing saw were found to perform poorly compared to similar shadow mask sensors not subjected photoresist coating that were partially diced (pre-scribed) prior to fabrication. Several methodologies were attempted in removing any residual photoresist from the sensor surfaces. Continued solution in acetone and application of ultrasonic in acetone solution were both tried with little change in results. A typical solution to such a problem is to use an oxygen plasma clean to remove such residual photoresist. However, due to the nature of the films that were depositing, there was a small percentage of Na in the resulting films that precluded the employment of this oxygen plasma system as this was designated a MOS piece of equipment that should be free of exposure to salt containing films. Surprisingly, it was discovered that when the sample substrates were exposed to an oxygen annealing in a tube

furnace after each photoresist step, residual photoresist was removed. This higher temperature process of about 400° C. removed the residual resist on the surface or in the pores of the films on the sensors. Sensors fabricated using this method produced the same or better results compared to equivalent shadow mask sensor arrays validating the employment of oxygen anneal to remove residual photoresist.

FIG. **12** is an optical image comparing arrays of sensors from hand fabricated down to photoresist based sensors. Each successive version of the sensor array is smaller in size, moving from the original hand built sensor array to the shadow mask version to the final photoresist-based version. As can be seen in FIG. **12**, the photoresist sensor is over a magnitude smaller in each dimension compared to the hand fabricated version. The reduction in size allows for smaller heater stages to be used to heat the sensor and thus reduced power requirements.

Sensor Performance—Shadow Mask

Sensors were tested at temperatures ranging from 500 to 600 degrees Celsius to determine the efficacy of the sensors. Generally sensors were found to work best when operated between 550 and 600 degrees Celsius. The sensors were tested by bringing the sensors to temperature and awaiting the sensor's stabilization. Once the temperature was stable, various NO gas concentrations were introduced to the sensor. Air was generally used as the baseline gas for these experiments. In general, the electrical connections to the sensors were made via either probe tips or wires attached to the contact pads at either end of the sensor array.

Test results of the initial first generation design are shown in FIG. **13**. The tested sensor was a five sensor array. As can be seen from the results, the sensor response at 50 ppm was less than 10 mV for this concentration of NO. A photographic image of one of the sensors in this array is shown in FIG. **8**. For comparison in FIG. **14**, the results of testing on a second generation shadow mask design are shown for a five sensor array. This second generation five sensor array shows a response of nearly 10 mV for a 33 ppm concentration of NO. It can be deduced from these measurements that the sensor response increased quite significantly (showing an equivalent response for a concentration reduction of 1.5 times) due to the changes made from the first to the second generation shadow mask design. Also shown in FIGS. **9&10** are photographic images of two sensors, showing the two different designs of the sensor in the second generation design. FIG. **15** shows the results of testing with a 10 sensor array from this same wafer. The results are shown for the sensor tested at 550 degrees Celsius.

In addition it was found that sensor response of each individual sensor in the array could be maximized by applying and/or modifying several parameters. For the working electrode minimizing the Pt exposed on the YSZ and maximizing WO_3 film exposure were found to increase the sensor response for a given NO concentration. Pt exposure on YSZ was minimized at both the reference and working electrodes. This change was done to minimize the triple point boundaries between the gas, Pt, and YSZ and thus the reactions at the exposed Pt surfaces on YSZ, thereby decreasing competing reactions that would decrease the induced potential across the sensor. Similarly, it was found that maximizing the WO_3 film on top of the YSZ was found to increase the induced potential across the sensor. In this case, this was due to an increase in the number of triple-point boundaries between the gas, WO_3, and YSZ.

Sensor Performance—Photoresist

The results of the photoresist-based version are shown in FIG. **16**. As can be seen in the test results, the photoresist-based version of the sensor array was capable of reaching below 500 ppb. These results are from a sensor array of 15 sensors connected in series on a chip. These sensors were tested using a catalytic filter to improve signal response and remove possible interfering gases.

The results of the testing on these various generations of designs indicate that the changes that were made between each generation were indeed beneficial to the overall performance of the sensor. Reducing the exposed Pt on the YSZ and increasing the WO3 covering the YSZ improved the sensitivity of the sensor as can be seen in comparing the results of the first and second generation shadow mask designs. The resulting design changes were applied to the photomask-based design, which is basically the second generation shadow mask design that was a factor of 0.35 in size compared to the shadow mask design. The test results of the photoresist design indicate that the sensor device is capable of at least 500 ppb level sensitivity and lower.

It was found during testing of the sensor arrays is the increased impedance of the connected connector array. In general, the 15 sensor array was found to be in the 60 MOhm range at operating temperature. The high impedance made the sensor array very sensitive to electrical Noise in the surrounding environment. A thicker YSZ film can decrease the impedance of the sensor due to the thicker film increasing the area through which ions could move from one end to the other of the sensor, however, it is found that the residual stress in the YSZ film increases and at higher thicknesses this stress can cause cracking in the film, especially after a thermal exertion to the operating temperature of the sensor. These cracks often run through the film, as seen in FIGS. **24***a*-**24***d*, and could possibly result in lower conductivity of the film.

Another possible issue is the longevity of the sensors. Although the sensors were capable of repeated performance during testing it was found that over a longer period of time (several days of continuous testing) that the sensor performance would gradually decrease. From optical and SEM examination it appears that the films may be reacting at temperature and migrating from their original deposited locations.

Although the invention has been described with reference to several specific embodiments, this description is not meant to be construed in a limited sense. Various modifications of the disclosed embodiments, as well as alternative embodiments of the invention will become apparent to persons skilled in the art upon the reference to the description of the invention. It is, therefore, contemplated that the appended claims will cover such modifications that fall within the scope of the invention.

Having described the invention, we claim:

1. A method of sensing gas, the method comprising:

receiving an original sample; and

generating a potential difference in a microfabricated potentiometric sensor device in response to presence of gas in the sample, wherein the microfabricated potentiometric sensor device comprises:

a base substrate;

an electrolyte layer disposed on the base substrate;

a plurality of potentiometric sensor units connected in series and coupled to the base substrate, each potentiometric sensor unit comprising:

an electrolyte layer disposed on the base substrate;

a two-part sensing electrode comprising a layer of tungsten oxide (WO_3) disposed on a platinum (Pt) contact;

a reference electrode comprising platinum (Pt);

wherein the ratio of the surface area of the tungsten oxide (WO_3) of the sensing electrode disposed on the electrolyte to the surface area of the Pt of the reference electrode disposed on the electrolyte is at least 2 to 1.

2. The method of claim **1**, comprising:

determining a level of gas within the original sample based on the potential difference generated by the microfabricated potentiometric sensor; and

wherein the sensor device determines the gas level at a sensitivity of at least 1 ppm.

3. The method of claim **2**, wherein the gas is NOx.

4. The method of claim **1**, wherein the electrolyte layer comprises yttria-stabilized zirconia (YSZ).

5. The method of claim **1**, wherein the sensor device comprises 15 to 20 sensor units.

6. A method of sensing gas, the method comprising:

receiving an original sample; and

generating a potential difference in a microfabricated potentiometric sensor device in response to presence of gas in the sample, wherein the microfabricated potentiometric sensor device comprises:

a base substrate;

an electrolyte layer disposed on the base substrate;

a plurality of potentiometric sensor units connected in series and coupled to the base substrate, each potentiometric sensor unit comprising:

an electrolyte layer disposed on the base substrate;

a two-part sensing electrode comprising a layer of tungsten oxide (WO_3) disposed on a platinum (Pt) contact; and

a reference electrode comprising platinum (Pt);

wherein the ratio of the surface area of the WO_3 sensing electrode disposed on the electrolyte to the surface area of the Pt reference electrode disposed on the electrolyte is sufficiently high such that the microfabricated potentiometric sensor device is capable of detecting the gas level at a sensitivity of at least 1 ppm.

7. The method of claim **6**, wherein the gas is NOx.

8. The method of claim **6**, wherein the electrolyte layer comprises yttria-stabilized zirconia (YSZ).

9. The method of claim **6**, wherein the sensor device comprises 15 to 20 sensor units.

* * * * *